Organic & Biomolecular Chemistry

Dynamic Article Links

Cite this: DOI: 10.1039/c2ob26630j

www.rsc.org/obc

PAPER

# pH Induced dual "OFF–ON–OFF" switch: influence of a suitably placed carboxylic acid†

**Kalyan K. Sadhu,[a] Shin Mizukami,[a,b] Akimasa Yoshimura[a] and Kazuya Kikuchi*[a,b]**

***Received 7th June 2012, Accepted 21st September 2012***
**DOI: 10.1039/c2ob26630j**



The design and synthesis of molecular probes competent for pH signaling within or beyond a certain range is a complicated matter. Herein a new mechanism for "OFF–ON–OFF" absorbance and fluorescence intensities *vs.* pH behaviour is described. The probe design is based on the connection of carboxylic acid derivatized benzoxazole and 7-hydroxycoumarin/iminocoumarin parts. The protonation/deprotonation of the carboxylic acid (–COOH), N atom of benzoxazole ring and hydroxy part of the coumarin ring have been used for this mechanistic study. We have designed the molecule in such a fashion that deprotonation of the hydroxy part takes place at a lower p$K_a$ compared to deprotonation of the –COOH. The dual "OFF–ON–OFF" properties of our probes depend on the C–C bond between the two different heterocyclic parts. Quantum mechanical calculations showed that the particular 'C–C' bond has an additional π-character. The twisting around this bond in different forms is responsible for such an "OFF–ON–OFF" property. This mechanism is new in fluorescence alteration processes. The delocalization of charge from one heterocyclic part to the other heterocyclic part in the mono- and dianionic forms controls the "OFF–ON–OFF" properties. The role of the carboxylic acid group was examined using an acetyl substituted derivative. One of our probes was successfully applied in live cell imaging studies in media at different pH.

## Introduction

Several biological processes have an effect on the intracellular or extracellular pH. For cellular diagnosis, numerous fluorogenic pH probes have been developed to estimate intracellular pH.[1] Recent research also pursues activatable probes for acidic and neutral pH.[2]

The most common technique for fluorescence enhancement at acidic pH involves the blocking of the photoinduced electron transfer (PET) process of dialkylamine based probes.[3] In another example, a phenyl ring plays the role of fluorescence quencher in basic medium.[4] Fluorescence turn-on with protonation around physiological pH was achieved by a pentamethine cyanine dye with p$K_a$ 7.5.[5] Recently, the direct correlation between the emission of a fluorescein based probe and its proton equilibria over a wide pH range was established.[6] The difference between the fluorescence properties of iminocoumarin and coumarin probes revealed strong fluorescence for iminocoumarin in acidic and neutral solutions, but little fluorescence for coumarin over a wide pH region, except under highly acidic conditions.[7]

The pH dependent fluorescence properties of umbelliferone[8] and 3-(2-benzoxazolyl)umbelliferone[9] (**U** and **BU** respectively, Chart 1) revealed the fluorescence "ON" state in basic medium due to loss of a proton from the phenolic hydroxy group. Systems competent for fluorescence "OFF–ON–OFF" by variation of pH are particularly important for the direct visualization of pH windows with implications in the life sciences. However, there have been only a few reports with such pH windows based on molecular probes.[6,10] Most of these previously reported pH sensitive molecules involved protonated pyridines (acting as electron acceptors in the PET process) and unprotonated tertiary

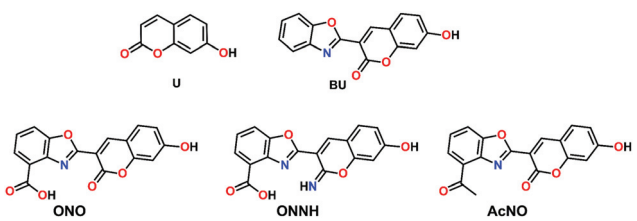


**Chart 1** Chemical structures of the probes **U**, **BU**, **ONO**, **ONNH**, and **AcNO**.

[a]*Division of Advanced Science and Biotechnology, Graduate School of Engineering, Osaka University, 2-1 Yamadaoka, Suita, Osaka 565-0871, Japan. E-mail: kkikuchi@mls.eng.osaka-u.ac.jp, http://www-molpro.mls.eng.osaka-u.ac.jp/; Fax: (+81) 6-6879-7875*
[b]*Immunology Frontier Research Center, Osaka University, 3-1 Yamadaoka, Suita, Osaka 565-0871, Japan*

†Electronic supplementary information (ESI) available: Experimental and theoretical details, UV–visible absorption spectra, and fluorescence spectra of the probes. See DOI: 10.1039/c2ob26630j

amines (acting as electron donors in the PET process). The presence of both functional groups within a multicomponent system generates several equilibria in the medium. The p$K_a$ values of such protonated functional groups cover different pH regions. Some probes contain coordinative interactions to gain such fluorescence properties. The deprotonation of the phenolic hydroxy group was mostly explored for the basic pH region. However, deprotonation of the carboxylic acid group in fluorescence-based pH modulation remains unexplored. Herein, our target was to develop a new pH sensor on the basis of deprotonation of the carboxylic acid group and also the influence of its position in the probe. In our probe design, we combined the carboxylic acid and phenolic hydroxy group together for pH monitoring. We synthesized 4-carboxylic acid-substituted coumarin and iminocoumarin derivatives (**ONO** and **ONNH**, Chart 1) for monitoring the effect of a wide range of pH.

## Results and discussion

### Design and synthesis

Since the development of **BU**, there have been some reports of 5-substituted derivatives including a carboxy group.[11] However, there has been only one report of a 4-substituted **BU** derivative.[12] In our design a 4-substituted acid derivative was chosen to study the influence of the nitrogen of the benzoxazolyl part in the vicinity during the deprotonation process.

In these probes, three protonation/deprotonation processes occur, one from the hydroxy group of the 7-hydroxycoumarin part and the others from the carboxylic acid and N atom of the substituted benzoxazolyl part. These two heterocyclic rings are connected *via* a 'C–C' bond. In order to compare the role of the –COOH in the dual spectroscopic modulation, our aim was to synthesize another 4-substituted derivative having a similar electronic effect without any protonation/deprotonation properties. The acetyl substituted aniline derivative showed a similar electron withdrawing effect compared to the acid analogue.[13–15] For our purpose, a new acetyl substituted **AcNO** (Chart 1) probe was also synthesized, where acetyl substitution played a significant contribution to the fluorescence properties compared to the carboxy group.

### Absorption studies of the probes

The absorbance spectra of **ONO** probe were monitored in 100 mM sodium phosphate buffers of different pH. An absorption maximum at 360 nm was observed for pH 4.8 (Fig. 1a). With increasing pH, another new absorption maxima appeared at 415 nm (pH 6.2, Fig. 1a). The absorption intensity increased at 415 nm with further increase of pH. A clear isosbestic point was obtained at 387 nm. This process involved the first deprotonation step of the neutral **ONO** probe. The absorption peak position remained in the same position within a certain pH range (7.8–8.9). With further increase in pH, a second deprotonation took place and this resulted in a slight blue shift of the absorption peak to 405 nm with low extinction coefficient (Fig. 1b).

A similar type of absorption profile was obtained for the **ONNH** probe. The absorption maximum of this iminocoumarin probe was obtained at 385 nm for pH 4.8 (Fig. S4a†). The

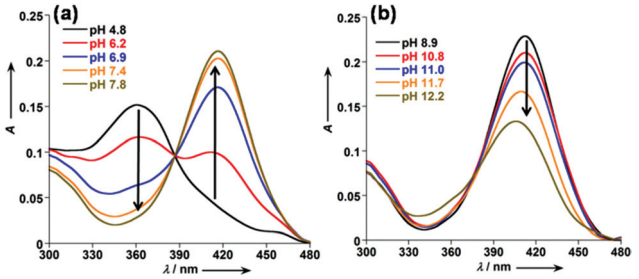


**Fig. 1** Absorption spectra of 10 μM **ONO** were measured in 100 mM sodium phosphate buffer containing 1% DMSO at various pH values (a) pH 4.8–7.8 and (b) 8.9–12.2 at 25 °C.

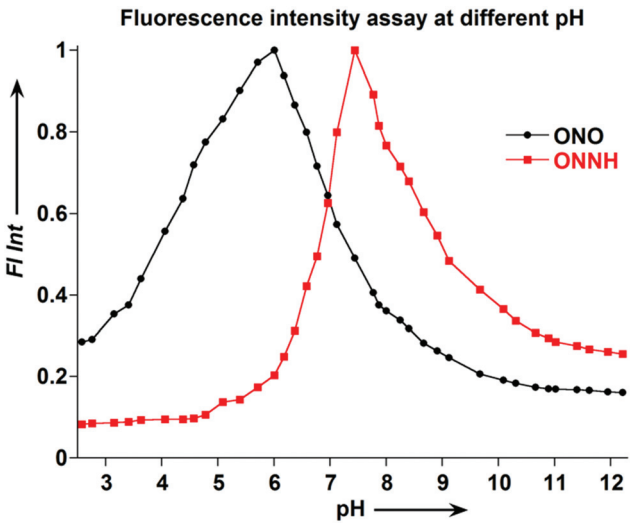


**Fig. 2** Relative fluorescence intensities of **ONO** at 470 nm ($\lambda_{ex}$ = 415 nm) and **ONNH** at 480 nm ($\lambda_{ex}$ = 435 nm) in 100 mM sodium phosphate buffer containing 0.1% DMSO at various pH values (2.6–12.2) at 25 °C.

absorption peak was shifted to 435 nm after the first deprotonation step with an isosbestic point at 399 nm. After the second deprotonation, the peak was blue shifted to 400 nm with low extinction coefficient (Fig. S4b†). The pH dependent absorption intensities at 415 nm and 435 nm for **ONO** and **ONNH** respectively (Fig. S5†) revealed absorption "OFF–ON–OFF" properties for both the probes.

The ground state p$K_1$ and p$K_2$ values (6.6 and 11.3 for **ONO**, 6.6 and 11.0 for **ONNH**) were obtained from the absorption spectra. These p$K_a$ values are the result of electronic charge distributions during the deprotonation process of the acidic form and its conjugated base in the ground state.

### Steady state emission studies of the probes

The fluorescence spectra of the **ONO** probe showed maximum emission at 470 nm ($\lambda_{ex}$ = 415 nm) in acidic pH. The fluorescence intensity at 470 nm was monitored at different pH ranging from acidic to basic (Fig. 2). The fluorescence intensity increased from pH 2.6 to 6.0, but with further increase in pH the fluorescence intensity decreased in a continuous manner. In the

case of the **ONNH** probe, a similar type of fluorescence assay was obtained by monitoring the emission at 480 nm ($\lambda_{ex}$ = 435 nm). The maximum fluorescence intensity was obtained at pH 7.4 for **ONNH**. At extremely basic pH, the emission maxima for both the probes were blue shifted and obtained at 450 nm (Fig. S6†). The fluorescence properties of both the probes showed an "OFF–ON–OFF" trend within a wide pH range. The stability of the probes was examined by analytical HPLC at different pH to overrule the immediate degradation of the probes (Fig. S8†).

The charge distributions of the acidic form and its conjugated base pair in the excited states are expected to be different from the ground states. These differences are reflected in the variation of acidity ($pK_a^*$) in the excited states. The $pK_a^*$ values were calculated by Förster cycle[16] and were found to be 4.7 and 7.7 for **ONO**, and 6.5 and 8.4 for **ONNH**. In the presence of biologically important metal ions, the fluorescence properties of these probes remained unaltered at different $pK_a^*$ values.

The differences in the second $pK_a$ and $pK_a^*$ values for both the probes were reflected in the fluorescence and absorption spectral changes at higher pH range. The position of the emission bands were blue shifted for both the probes around pH 10.8. On the other hand, similar kinds of shift for the absorption spectra were observed around pH 11.7 for both **ONO** and **ONNH**. These changes in the spectra account for the second deprotonation step.

The contribution due to different prototropic zwitterionic forms[17] around the heterocyclic part in the solution also plays an important contribution in the $pK_a^*$ determination. Similar types of observation have been reported in the literature.[18] The contribution from these prototropic forms is also reflected in the mismatch of the absorbance and excitation spectra.

The dissociation constant in the excited state includes the favorable excited state intramolecular proton transfer (ESIPT)[19] from the proton of the carboxy group to the benzoxazolyl nitrogen atom. ESIPT could also be a possibility for modulation of fluorescence properties due to the presence of H-chelate ring[19c] as a reaction center.

In order to study the participation from the carboxylic acid proton in the spectral "OFF–ON–OFF" properties, we studied the spectral properties of the **AcNO** probe containing a 4-acetyl substituted derivative. The absorbance and fluorescence properties of the **AcNO** probe showed similar types of "OFF–ON" spectral patterns (Fig. S10†) to those of **BU**.[9] These differences bring forward the vital role of the acid groups in the "OFF–ON–OFF" spectral properties of the **ONO** and **ONNH** probes. No spectral change for **AcNO** at higher pH suggested the absence of a second deprotonation of this probe.

### Fluorescence lifetime studies of the probes

In order to check the origin of the "OFF–ON–OFF" spectral properties of the probes, fluorescence decay profiles of both the probes were monitored around different $pK_a^*$ values (Fig. S12†). In the case of **ONO**, the trend in nonradiative decay rate constant values ($k_{nr}$, Fig. 3) around two different $pK_a^*$ confirmed the maximum rigid geometry in the monoanionic form. The $k_{nr}$ values were reached to the maximum within the two $pK_a^*$ regions of **ONO** probe. On the other hand, $k_{nr}$ values for **ONNH** were almost constant (Fig. 3) around different $pK_a^*$ regions. This indicates that there is no significant change in geometry around $pK_a^*$ for **ONNH** probe.

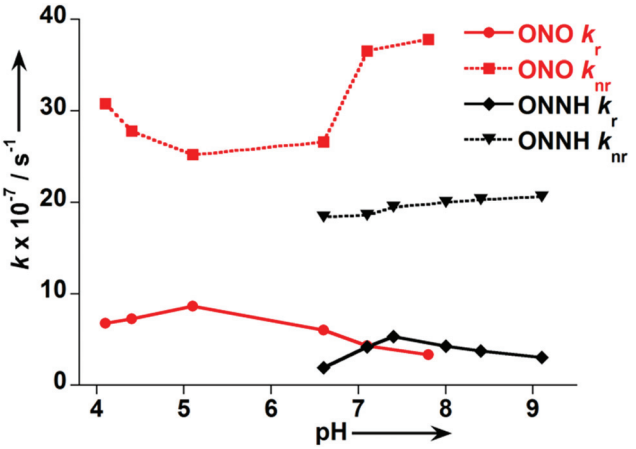


**Fig. 3** Radiative and nonradiative decay rate constants of **ONO** and **ONNH** at different pH around two different $pK_a$.

The trend of radiative decay rate constants ($k_r$) for both the probes (Fig. 3) around different $pK_a^*$ values controlled the fluorescence "OFF–ON–OFF" modulation. The delocalization of the negative charge between the two heterocyclic parts in the monoanionic form was responsible for the "OFF–ON" state. The second deprotonation from the benzoxazolyl part restricted the negative charge delocalization from the hydroxycoumarin part. This resulted in a further fluorescence "OFF" state.

### Mechanism of the fluorescence "OFF–ON–OFF": theoretical support

It is a well-established phenomenon that the deprotonation of carboxy group occurs at lower pH compared to phenolic proton.[20] To rationalize the pH profile of the newly synthesized probes in the same fashion, deprotonation of the carboxy group was considered during the first deprotonation step (**ONO$_1$′**, Scheme 1). However, the changes in the spectral properties could not be correlated with this deprotonation. Possibly hydrogen bonding between the carboxylic acid and the N atom of the benzoxazolyl part restricted the deprotonation of the carboxylic acid. The protonated zwitterionic form (benzoxazolium ion **ONO-z**, Scheme 1) could also play an important role in the spectral properties.

In order to check out these possibilities, theoretical calculations for optimized geometries were carried out at the B3LYP/6-31G++ level of theory in Hartree–Fock method using the Gaussian 09W programme package.[21] The energies of the optimized geometries in the zwitterionic form (**ONO-z**) were found to be comparable with that of **ONO** (Scheme 1). Electron density calculations ruled out the possibility of deprotonation of the carboxylic acid during the first deprotonation (Fig. 4a). This calculation suggested that the first deprotonation was possible from the 7-hydroxy group of the coumarin instead of the carboxylic acid. The favorable interaction of the carboxylic acid

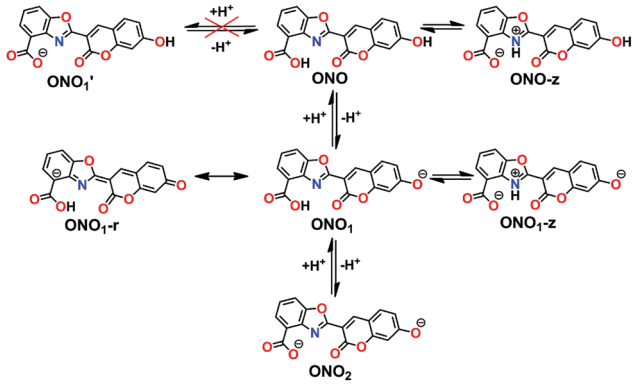


**Scheme 1** Probable protonation equilibria of **ONO**.

proton with the nitrogen atom of the heterocyclic ring was involved with the poor acidity of the carboxylic acid proton. The absence of a pH dependent fluorescence "OFF–ON" switch in the case of 7-methoxy-substituted coumarin[22] also indirectly confirmed the first switching mechanism to be from the 7-hydroxy coumarin part of the newly synthesized probes.

Optimized geometry depicted the nature of the bond order between the two heterocyclic parts as 1.5, with a calculated 'C–C' bond distance of 1.45 Å. Contour π-MO of the neutral planar form of **ONO** (Fig. 4b) depicted a "C⋯C" bond instead of 'C–C' between the benzoxazolyl part and the 7-hydroxy-coumarin part. The deprotonation of the 7-hydroxycoumarin part could lead to formation of a stable quinoid geometry by resonance (**$ONO_1$-r**, Scheme 1). The first "OFF–ON" absorption profile of **ONO** during the first deprotonation (Fig. 1a) was similar to the absorption profile of **BU**.[9] However, unlike **BU**, the second "OFF" absorption state of **ONO** was observed with further increase in pH due to the loss of proton from the carboxylic acid (**$ONO_1$**) or benzoxazolium ion (**$ONO_1$-z**) to form **$ONO_2$** as shown in Scheme 1.

The result obtained from the fluorescence lifetime experiment has been further supported by the different energy minimized structures of twisted and planar geometries of **ONO** in different ionic and neutral forms (Fig. 5 and Fig. S13–S15†). The twisted geometry in the neutral state became planar after the first deprotonation. Further deprotonation generated the twisted dianionic form. These geometries were responsible for the $k_{nr}$ values of **ONO**. On the other hand, the planar geometries of different ionic and neutral species of **ONNH** (Fig. 5) were responsible for the constant $k_{nr}$ values in the different forms. The planar geometries in the case of **ONNH** originated from the hydrogen bond between the imine group and the heteroatom of the benzoxazolyl part.

The calculated electronic charge distribution on the heteroatoms (N and O) of the benzoxazolyl part in the neutral and ionic states (Table S1†) supported the variation in the $k_r$ values for both the probes. The charge densities on these heteroatoms in the monoanionic forms are first increased from the neutral states due to the favorable charge delocalization process. However, the values are then decreased in the dianionic forms due to the restriction in the delocalization process across the "C⋯C" bond. This is reflected in the maximum $k_r$ values in the monoanionic forms for both **ONO** and **ONNH** probes.

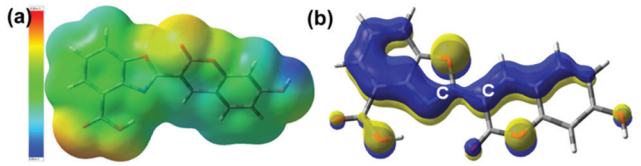


**Fig. 4** (a) Calculated electron density contour surface (blue: positive electrostatic potential, and red: negative electrostatic potential) of **ONO** and (b) contour π-MO surface of planar ground state form of **ONO** showing the origin of the "C⋯C" bond.

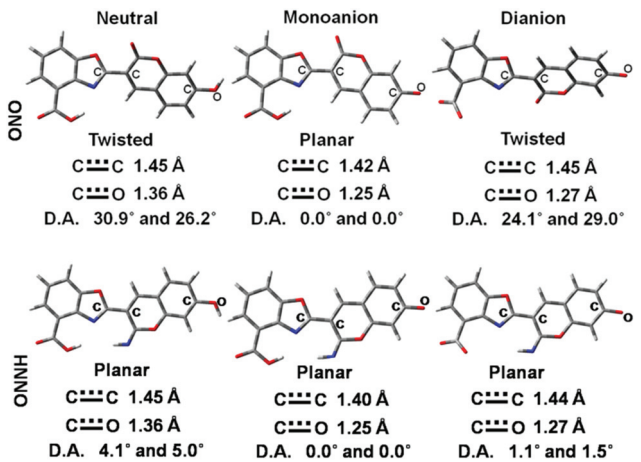


**Fig. 5** The energy-minimized ground state geometries of **ONO** and **ONNH** in neutral, monoanion, and dianionic forms along with the dihedral angle (D.A.) between the benzoxazolyl part and the coumarin part.

In order to correlate the experimental absorption spectra of the probes at different pH, the transition energies of the optimized geometries were calculated by time-dependent density functional theory (TD-DFT) using the same level of basis set. TD-DFT calculations for different species (Fig. S15†) also supported the experimentally observed red and blue shifts of the probes.

### Live cell imaging studies with ONNH probe

We have applied the **ONNH** probe to evaluating its applicability for live cell imaging studies by confocal microscopy. Fluorescence images of the living HEK293T cells were taken after probe treatment in different extracellular pH buffers (Fig. S16†). The highest fluorescence intensity was observed at pH 7.4. The fluorescence images at pH 6.5 and 8.0 confirmed the fluorescence "OFF–ON–OFF" of **ONNH** probe in living cell imaging studies.

## Conclusions

In conclusion, we have developed a new mechanism for a reversible dual "OFF–ON–OFF" pH sensor with the influence from a suitably located carboxylic acid group. The deprotonation of a carboxylic acid group or benzoxazolium ion was used for the first time in the alteration of absorption and fluorescence properties simultaneously. Theoretical study supported the trend of the

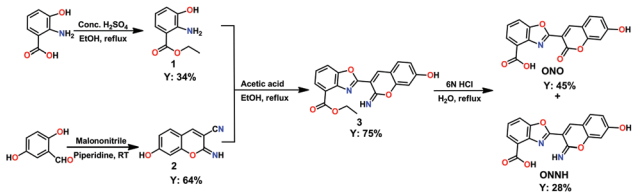


**Scheme 2** Synthetic route to **ONO** and **ONNH**.

kinetic parameters obtained from experimental studies. In addition, the iminocoumarin probe **ONNH** showed the maximum fluorescence at physiological pH conditions and has been successfully applied in live cell imaging studies.

## Experimental section

See ESI† for full experimental details and other supporting materials.

The synthetic route for the **ONO** and **ONNH** is illustrated in Scheme 2.

Synthesis of **1**. Compound **1** was synthesized according to the procedure available in the literature.[23]

Synthesis of **2**. Compound **2** was synthesized according to the procedure available in the literature.[24]

Synthesis of **3**. Compound **2** (186 mg, 1 mmol) was added to an ethanol solution (15 mL) of **1** (182 mg, 1 mmol). Acetic acid (1 mL) was added to this mixture. The mixture was then set for reflux at 90 °C. After 24 h the desired product was isolated by flash column chromatography using 9% methanol in dichloromethane. Compound **3** was isolated as a yellow solid after complete removal of solvent (263 mg, y. 75%). $^1$H NMR ($CD_3OD$, 400 MHz) $\delta$ 1.38 (t, 3H), 4.33 (q, 2H), 6.43 (d, 1H), 6.61 (s, 1H), 7.51 (m, 1H), 7.60 (d, 1H), 7.92 (d, 1H), 7.99 (d, 1H), 8.35 (s, 1H); $^{13}$C NMR ($CD_3OD$, 100 MHz) $\delta$ 14.4, 63.0, 60.3, 103.7, 107.8, 108.4, 115.9, 118.0, 123.5, 126.8, 129.6, 130.3, 140.9, 142.3, 148.1, 151.6, 155.7, 157.4, 163.9, 168.2; HRMS ($C_{19}H_{15}N_2O_5$, FAB+); Found 351.0992; Calc. 351.0981.

Synthesis of **ONO** and **ONNH**. Compound **3** (20 mg, 0.06 mmol) was added to an aqueous medium (10 mL) containing 6N hydrochloric acid. The mixture was then set for reflux at 100 °C. The reflux was continued for 2 h. The desired products **ONO** (8 mg, y. 45%) and **ONNH** (5 mg, y. 28%) were isolated using preparative HPLC.

**ONO** characterization: $^1$H NMR (DMSO-$d_6$, 400 MHz) $\delta$ 6.83 (s, 1H), 6.89 (d, 1H), 7.09 (d, 1H), 7.15 (dd, 1H), 7.22 (d, 1H), 7.84 (d, 1H), 8.90 (s, 1H), 9.90 (br, 1H), 10.95 (br, 1H); $^{13}$C NMR (DMSO-$d_6$, 100 MHz) $\delta$ 100.4, 102.1, 111.4, 113.3, 114.8, 119.1, 119.3, 120.7, 126.2, 132.6, 148.2, 149.4, 150.8, 156.8, 160.4, 161.4, 164.2; HRMS ($C_{17}H_{10}NO_6$, FAB+); Found 324.0502; Calc. 324.0508.

**ONNH** characterization: $^1$H NMR (DMSO-$d_6$, 400 MHz) $\delta$ 6.87 (s, 1H), 6.97 (d, 1H), 7.24 (d, 1H), 7.35 (dd, 1H), 7.55 (d, 1H), 7.73 (d, 1H), 9.53 (s, 1H), 9.63 (s, 1H), 11.21 (s, 1H), 11.84 (s, 1H); $^{13}$C NMR (DMSO-$d_6$, 100 MHz) $\delta$ 99.9, 107.5, 116.7, 124.8, 125.8, 128.2, 133.6, 134.8, 138.6, 141.1, 146.7, 148.4, 153.1, 161.7, 165.5, 169.8, 173.3; HRMS ($C_{17}H_{11}N_2O_5$, FAB+); Found 323.0680; Calc. 323.0668.

The synthetic route for **AcNO** is illustrated in Scheme 3.

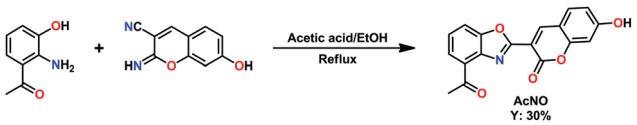


**Scheme 3** Synthetic route to **AcNO**.

Synthesis of **AcNO**. Compound **2** (9 mg, 0.05 mmol) was added to an ethanol solution (15 mL) of 3′-hydroxy-2′-aminoacetophenone (8 mg, 0.05 mmol). Acetic acid (1 mL) was added to this mixture. The mixture was then set for reflux at 90 °C for 24 h. The desired product **AcNO** was isolated using preparative HPLC (5 mg, y. 30%). $^1$H NMR (DMSO-$d_6$, 400 MHz) $\delta$ 2.68 (s, 3H), 6.33 (d, 1H), 6.80 (s, 1H), 6.90 (d, 1H), 7.39 (d, 1H), 7.48 (dd, 1H), 7.78 (d, 1H), 7.83 (d, 1H), 8.81 (s, 1H); $^{13}$C NMR (DMSO-$d_6$, 100 MHz) $\delta$ 28.2, 110.6, 112.3, 118.3, 122.3, 123.6, 126.9, 135.8, 138.5, 139.2, 143.6, 145.3, 149.9, 152.2, 156.8, 157.1, 162.3, 202.1; HRMS ($C_{18}H_{11}NO_5$, FAB+); Found 321.0642; Calc. 321.0637.

## Acknowledgements

This research is supported by MEXT of Japan (Grants 20675004 to K. K.), by CREST from JST, by Asahi Glass Foundation, by the Grant-in-Aid from the Ministry of Health, Labour and Welfare (MHLW) of Japan, and by the Japan Society for the Promotion of Science (JSPS) through its "Funding Program for World-Leading Innovative R&D on Science and Technology (FIRST Program)." We thank Dr Koushik Dhara of Osaka University for his helpful discussion and Prof. Hirohiko Houjou at the University of Tokyo for his suggestion regarding the quantum calculations. KKS and AY acknowledge GCOE Fellowship of Osaka University.

## References

1 (*a*) J. Han and K. Burgess, *Chem. Rev.*, 2010, **110**, 2709; (*b*) R. P. Haugland, *The Handbook – A Guide to Fluorescent Probes and Labeling Technologies*, Molecular Probes, Eugene, OR, 10th edn, 2005.
2 (*a*) T. Kowada, J. Kikuta, A. Kubo, M. Ishii, H. Maeda, S. Mizukami and K. Kikuchi, *J. Am. Chem. Soc.*, 2011, **133**, 17772; (*b*) W. F. Jager, T. S. Hammink, O. V. D. Berg and F. C. Grozema, *J. Org. Chem.*, 2010, **75**, 2169; (*c*) Y. Urano, D. Asanuma, Y. Hama, Y. Koyama, T. Barrett, M. Kamiya, T. Nagano, T. Watanabe, A. Hasegawa, P. L. Choyke and H. Kobayashi, *Nat. Med.*, 2009, **15**, 104; (*d*) S. Uchiyama and Y. Makino, *Chem. Commun.*, 2009, 2646; (*e*) B. Tang, X. Liu, K. Xu, H. Huang, G. Yang and L. An, *Chem. Commun.*, 2007, 3726; (*f*) S. Yao, K. J. Schafer-Hales and K. D. Belfield, *Org. Lett.*, 2007, **9**, 5645; (*g*) A. P. de Silva, S. S. K. de Silva, N. C. W. Goonesekera, H. Q. N. Gunaratne, P. L. M. Lynch, K. R. Nesbitt, S. T. Patuwathavithana and N. L. D. S. Ramyalal, *J. Am. Chem. Soc.*, 2007, **129**, 3050.
3 D. Rehm and A. Weller, *Isr. J. Chem.*, 1970, **8**, 259.
4 G. Wenska and S. Paszyc, *Can. J. Chem.*, 1988, **66**, 513.
5 M. S. Briggs, D. D. Burns, M. E. Cooper and S. J. Gregory, *Chem. Commun.*, 2000, 2323.
6 (*a*) D. Buccella, J. A. Horowitz and S. J. Lippard, *J. Am. Chem. Soc.*, 2011, **133**, 4101; (*b*) B. A. Wong, S. Friedle and S. J. Lippard, *J. Am. Chem. Soc.*, 2009, **131**, 7142.
7 K. Komatsu, Y. Urano, H. Kojima and T. Nagano, *J. Am. Chem. Soc.*, 2007, **129**, 13447.
8 (*a*) D. Jacquemin, E. A. Perpète, G. Scalmani, M. J. Frisch, X. Assfeld, I. Ciofini and C. Adamo, *J. Chem. Phys.*, 2006, **125**, 164324; (*b*) R. H. Abu-Eittah and B. A. H. El-Tawil, *Can. J. Chem.*, 1985, **63**, 1173; (*c*) D. G. Crosby and R. V. Berthold, *Anal. Biochem.*, 1962, **4**, 349.

9 (*a*) A. E. H. Machado and J. A. Miranda, *J. Photochem. Photobiol., A*, 2001, **141**, 109; (*b*) O. S. Wolfbeis and E. Koller, *Microchim. Acta*, 1985, **1**, 389; (*c*) O. S. Wolfbeis, E. Koller and P. Hochmuth, *Bull. Chem. Soc. Jpn.*, 1985, **58**, 731; (*d*) O. S. Wolfbeis, E. Fuerlinger, H. Kroneis and H. Marsoner, *Fresenius' Z. Anal. Chem.*, 1983, **314**, 119; (*e*) A. H. Naik and S. Seshadri, *Indian J. Chem., Sect. B: Org. Chem. Incl. Med. Chem.*, 1977, **15B**, 506.

10 (*a*) G. Cavallaro, G. Giammona, L. Pasotti and P. Pallavicini, *Chem.–Eur. J.*, 2011, **17**, 10574; (*b*) Y. Chen, H. Wang, L. Wan, Y. Bian and J. Jiang, *J. Org. Chem.*, 2011, **76**, 3774; (*c*) P. Pallavicini, Y. A. Diaz-Fernandez and L. Pasotti, *Analyst*, 2009, **134**, 2147; (*d*) V. Amendola, C. Mangano and P. Pallavicini, *Dalton Trans.*, 2004, 2850; (*e*) T. Gunnlaugsson, J. P. Leonard, K. Sénéchal and A. J. Harte, *J. Am. Chem. Soc.*, 2003, **125**, 12062; (*f*) L. Fabbrizzi, F. Gatti, P. Pallavicini and L. Parodi, *New J. Chem.*, 1998, **22**, 1403; (*g*) A. P. de Silva, H. Q. N. Gunaratne and C. P. McCoy, *Chem. Commun.*, 1996, 2399.

11 L. M. Rodrigues, X. H. Luan, A. M. A. G. Oliveira and A. M. F. Olivera-Campos, *J. Chem. Res.*, 2004, 120.

12 K. U. Joseph and V. V. Somayajulu, *J. Indian Chem. Soc.*, 1979, **56**, 505.

13 A. N. Pankratov, I. M. Uchaeva, S. Y. Doronin and R. K. Chernova, *J. Struct. Chem.*, 2001, **42**, 739.

14 M. Y. Gokhale and L. E. Kirsch, *J. Pharm. Sci.*, 2009, **98**, 4639.

15 W. R. Sherman and E. Robins, *Anal. Chem.*, 1968, **40**, 803.

16 B. Marciniak, H. Kozubek and S. Paszyc, *J. Chem. Educ.*, 1992, **69**, 247.

17 N. Klonis and W. H. Sawyer, *J. Fluoresc.*, 1996, **6**, 147.

18 (*a*) J. R. Lakowicz, *Principles of Fluorescence Spectroscopy*, Springer Science+Business Media, LLC, 3rd edn, 2006; (*b*) A. Orte, L. Crovetto, E. M. Talavera, N. Boens and J. M. Alvarez-Pez, *J. Phys. Chem. A*, 2005, **109**, 734; (*c*) C. Burda, M. H. Abdel-Kader, S. Link and M. A. El-Sayed, *J. Am. Chem. Soc.*, 2000, **122**, 6720; (*d*) S. Hagopian and L. A. Singer, *J. Am. Chem. Soc.*, 1985, **107**, 1874.

19 (*a*) W. Klopffer, *Adv. Photochem.*, 1977, **10**, 311; (*b*) D. Huppert, M. Gutman and M. J. Kaufmann, *Adv. Chem. Phys.*, 1981, **47**, 643; (*c*) S. Lochbrunner, A. Szeghalmi, K. Stock and M. Schmitt, *J. Chem. Phys.*, 2005, **122**, 244315.

20 H. C. Brown, D. H. MaDaniel and P. Haflinger, *Determination of Organic Structures by Physical Methods*, ed. E. A. Braude, F. C. Nachod, Academic Press, New York, 1955.

21 M. J. Frisch, *et al.*, *GAUSSIAN 09 (RevisionA.02)*, Gaussian, Inc., Wallingford, CT, USA, 2009.

22 J. R. Heldt, J. Heldt, M. Stoń and H. A. Diehl, *Spectrochim. Acta, Part A*, 1995, **51**, 1549.

23 L. R. Morgan, J. D. M. Weimorts and C. C. Aubert, *Biochim. Biophys. Acta*, 1965, **100**, 393.

24 J. Volmajer, R. Toplak, I. Leban and A. M. L. Marechal, *Tetrahedron*, 2005, **61**, 7012.




 